Lasers in Manufacturing Conference 2017

Flexible, compact and picosecond laser capable four-beam interference setup

Alexander Peter[a,*], Volkher Onuseit[a], Christian Freitag[a], Sebastian Faas[a], and Thomas Graf[a]

[a]*Institut für Strahlwerkzeuge (IFSW), University of Stuttgart, Pfaffenwaldring 43, 70569 Stuttgart, Germany*

Abstract

Periodic micro structures on surfaces offer unique properties, such as hydrophobic behavior, holographic light reflection or friction and wear minimization. Multi-beam interference patterning is a technology to produce micro structures from several micrometers down to below 1 µm, dependent on the wavelength and angle between the interfering beams. A high power capable four-beam interference setup, designed for infrared ultrashort pulsed laser sources in the picosecond regime will be shown. The setup provides independent variation of the period, intensity distribution and pattern size of the interference pattern. The period is variable from 1 µm with a working distance of 100 mm up to 5 µm with a working distance of about 800 mm. The intensity distribution can be modified to different shapes, such as lines, holes, ripples etc. by controlling the polarization of each beam separately. The fluence of the pattern is controllable by changing the pattern size. To change the pattern size, the beam diameter can be varied by a telescope with variable focal length. The setup is built in a stable design of a size of about 300x300x300 mm³ and a weight of 4.6 kg. To avoid aberrations at high laser power, especially focus shift, the setup was designed with high reflective mirrors. An experimental verification shows the comparison between the experimental results and the calculated design and features.

Keywords: Direct Laser Interference Patterning; four beam interference; micro structuring; picosecond pulsed laser

* Corresponding author. Tel.: +49-711-685-69743.
E-mail address: alexander.peter@ifsw.uni-stuttgart.de.

1. Introduction

The interest in and the range of applications of micro and nano structures are currently increasing [Lasagni et al., 2015]. Chemical, mechanical or laser based technologies are possible to produce such structures. Direct laser interference patterning (DLIP) is one of the promising technologies, due to its advantages, like structuring areas in a one-step process, nearly arbitrary and material independent structure geometries. The feasibility and versatility of DLIP was demonstrated by A.Lasagni et al., 2014, A. Aktag et al., 2006, M. Campbel et al., 2000 and M. Steger and A. Gillner, 2016 only to mention a few.

The proposed setup was designed in the context of a project, researching hydrophobic surfaces on steel. Determining of structure properties requires a flexible setup to be able to produce a certain spectrum of different structures. In this work a setup is proposed that is designed to realize these requirements.

2. Layout of Four-Beam Interference Setup

2.1. Requirements and Theory

In the context of the project, researching hydrophobic surfaces, adjustable structure range of 1 to 5 µm and flexible structure forms like lines, cones or ripples are required. The pattern size needs to be adjustable to distribute different pulse energies to the most efficient fluence of $e^2 \cdot 0.1 \ \frac{\mathrm{J}}{\mathrm{cm}^2}$ [Neuenschwander et al., 2012]. Due to limited installation space the design had to be compact and stable enough to hold interference conditions during movements of the entire setup. Further the setup has to stand picosecond laser pulse energy of about 3 mJ. This demands resistant optical as well as mechanical design with flexible adjustments.

The presented setup is based on a four-beam-interference principle. The beams interfere at a certain angle of incidence at the sample surface plane. **Fehler! Verweisquelle konnte nicht gefunden werden.** (a) shows the applied symmetric arrangement type of the four-beam interference principle. In this arrangement, all four beams have the same angle of incidence and angle to the surface normal and form a cone with same distances to each other. This is necessary for a constant pattern in z-direction.

In the region where the beams overlap, they produce a certain interference pattern at the sample surface plane. The plot in **Fehler! Verweisquelle konnte nicht gefunden werden.** (b) shows the intensity distribution of the interference patterns on the surface of the sample. The scale of this plot is normed to the intensity of four overlapping beams of same power without interference effects. Cheng Lu and R. H. Lipson, 2010 write the intensity distribution of the interference pattern as:

$$I = \sum_{i} E_i^2 + \sum_{i<j}^{N} E_{ij}^2 \, \hat{e}_{ij}^2 \cos[K_{ij} \cdot r + \varphi_{ij}] \qquad (1)$$

where $E_{ij}^2 = |E_i E_j|, K_{ij} = k_i - k_j, \varphi_{ij} = \varphi_i - \varphi_j$ and $\hat{\mathrm{e}}_{ij} = |\hat{\mathrm{e}}_i \cdot \hat{\mathrm{e}}_j|$. E_j describes the electric field vector with

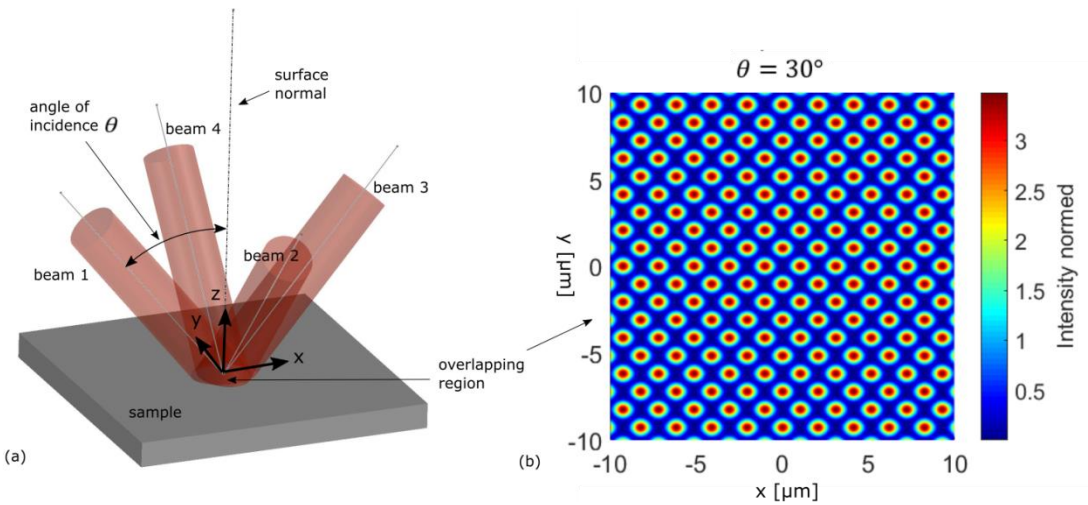

Fig. 1. Type of four beam interference principle. Orientation of the four interfering beams is symmetric and form a cone (a). The resulting interference at the overlapping region is a periodic pattern in the x,y-plane (b).

$$E_j = |E_j|\hat{e}_j \, e^{i(k_j \cdot r - \omega t + \varphi_j)} \tag{2}$$

where $|E_j|, \hat{e}_j, k_j$ and φ_j are the jth wave's amplitude, polarization vector, wave's vector and phase, respectively.

The patterns period Λ, shown in **Fehler! Verweisquelle konnte nicht gefunden werden.** (b), depends on the wavelength λ of the laser, angle of incidence θ and number of beams N. M. Steger and A. Gillner, 2016 showed, that for four beams interference pattern ($N = 4$) the period can be written as:

$$\Lambda = \lambda/(\sqrt{2}\, sin\, \theta) \tag{3}$$

The intensity distribution in **Fehler! Verweisquelle konnte nicht gefunden werden.** (b) is produced by linear polarization with same orientation of all four beams of 0° to the x axis. For three beams J. Huang et al., 2010 and for four beams A. Aktag et al., 2006 showed that relatively different polarizations of each beam influences the intensity distribution of the pattern.

Formula (1) contains the period variation by the angle of incidence as well as the intensity distribution influence of relative polarizations. To connect the interference pattern with the requirements for the surface the ablation of the interference pattern was calculated with formula (1).

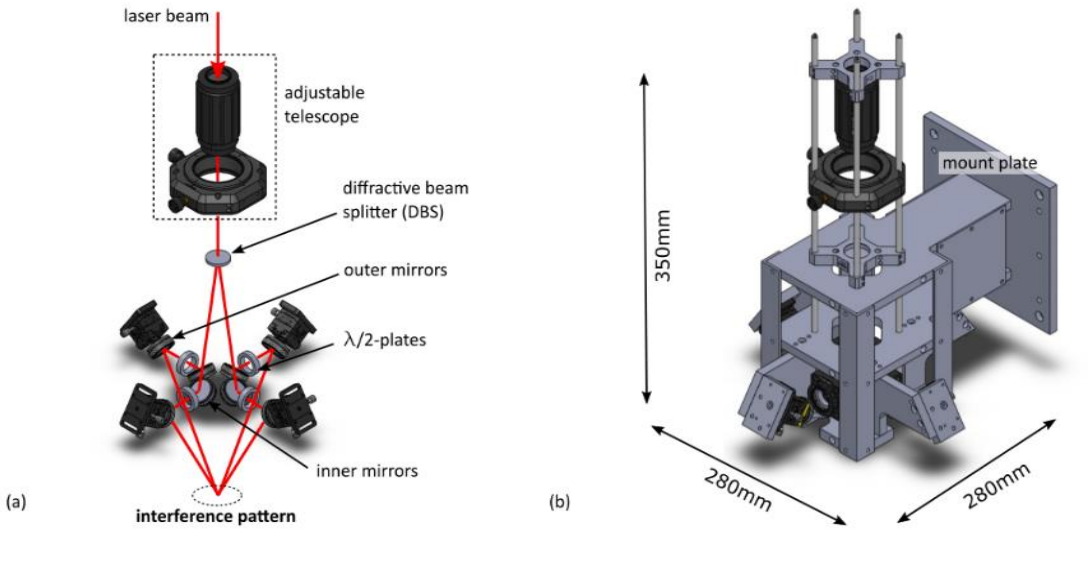

Fig. 1. Layout of four beam interference setup. Laser beam guidance with assistance of picosecond pulsed laser of the 1kW class capable optical elements (a) embedded into a stable construction of 10 mm aluminium plates (b).

2.2. Optical and mechanical Layout

To reduce thermal effects in transmitting optics with picosecond pulsed laser of 1kW class, the design based on reflective optics. Only the focusing telescope, DOE and the $\lambda/2$-plates are transmitting optics due to the requirements for the installation space. The described setup was designed for a wavelength of 1030 nm.

Fig. 1 (a) shows the layout of the setup. A single laser beam first passes the adjustable telescope and is then splitted into four beams by the diffractive optical element (DOE). After the DOE the four beams are reflected on four inner mirrors. From the inner mirrors the beams propagate through $\lambda/2$-plates onto outer mirrors, which deflect the beams onto the sample as illustrated in **Fehler! Verweisquelle konnte nicht gefunden werden.** (a). The mechanical tolerances and the adjustment is accurate enough to interfere 10ps pulses, with a coherence length under 3mm.

Except the linear dependence of the pattern diameter to the period, the layout of the setup provides three independent variable parameters. The period of the structures, intensity distribution and pattern size to adjust the fluence to the pulse energy of the laser pulse.

The period is controllable with the angle of incidence. Therefore the outer mirrors, which are responsible for the angle of incidence, are mounted on adjustable goniometers. In this case, the angle of incidence is variable from 5° to 45°. This corresponds to a structure period of 5 µm with a working distance of about 600 mm down to 1 µm with a working distance of about 80 mm, where the working distance is notated as the distance from the bottom of the setup to the crossing point of the beams.

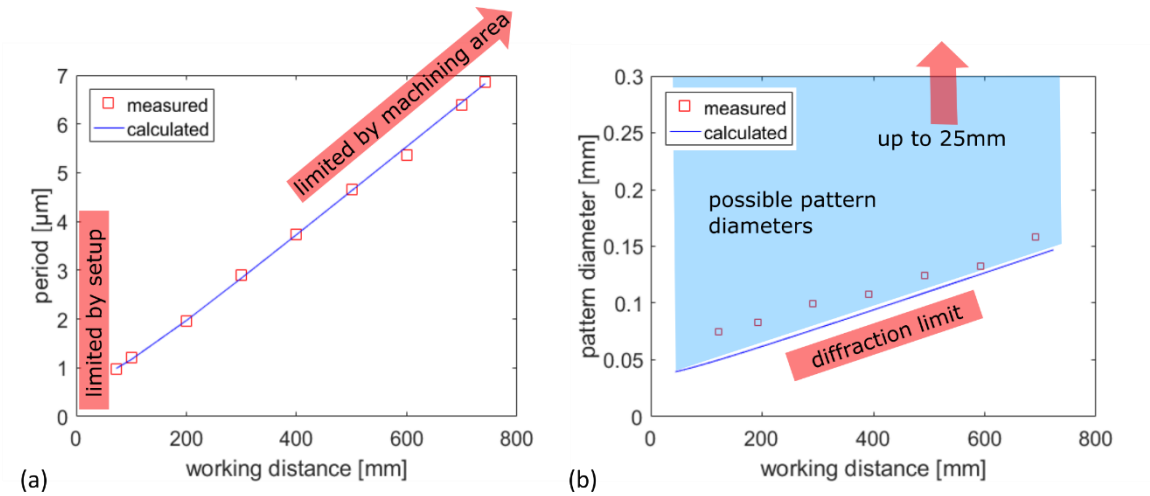

Fig. 2. Validation of period (a) and pattern size (b) adjustment versus working distance and angle of incidence respectively. Up and down limits are described and marked in red boxes.

The intensity distribution is defined by the polarization of each beam. The polarization can be adjusted with the $\lambda/2$-plates in every beam path. Some selected possible intensity distributions are shown in **Fehler! Verweisquelle konnte nicht gefunden werden.**.

To control the pattern size, divergence angle of the beams is variable with the telescope (Fig. 1). This was implemented with a Galilei telescope where the negative lens is longitudinal moveable in a lens tube.

The layout is embedded into a stiff construction of 10 mm aluminum plates, as shown in Fig. 1 (b). This avoids influences of mechanical vibrations to the interference patterns. The nearly cubic construction geometry provides stability in case of movements of the entire setup during processes.

3. Experimental Validation

This section describes the validation of the three variable parameters of the interference patterns. These three parameters are the period, intensity distribution and pattern size. For the validation a TruDisk 5050 Yb:YAG disk laser with 1030 nm wavelength, pulse duration below 10 picoseconds was used. The pulse energy was reduced to 5 µJ at a repetition rate of 3 kHz. With assistance of a 50x microscope objective the interference patterns were magnified and imaged onto a CMOS camera sensor of 768x576 pixels with a pixel size of 8.3 µm.

3.1. Period

The period depends on the angle of incidence that corresponds to the working distance. Figure 3 (a) shows the comparison of the measured to the calculated period versus the working distance. The blue curve was calculated with equation *(*3) with the proportional relation:

(4)

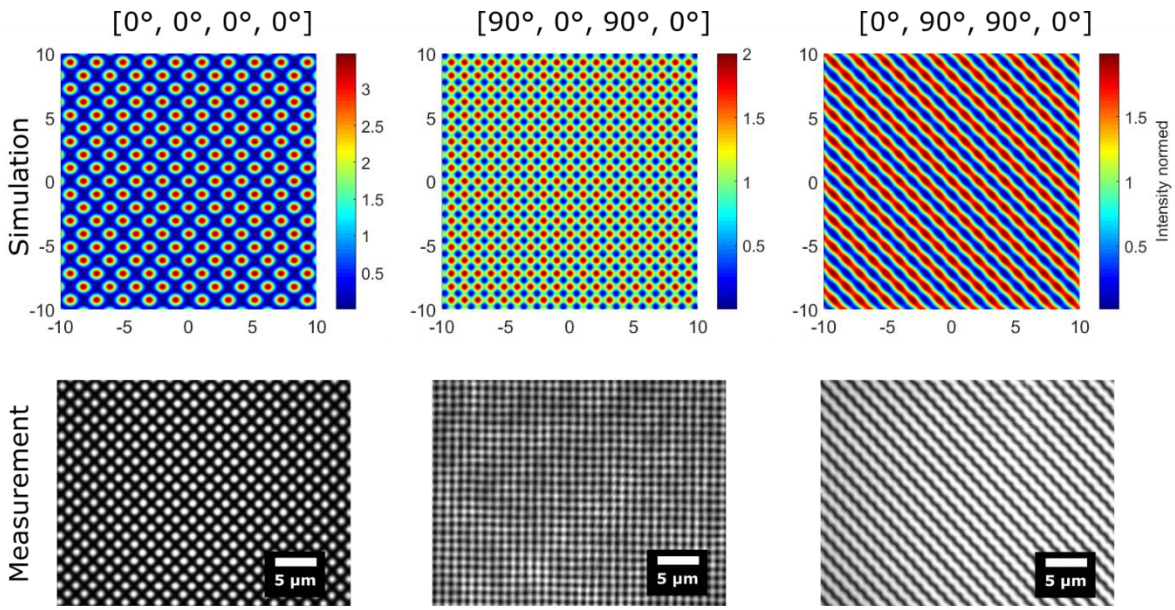

Fig. 3. Validation of selected three intensity distributions at an angle of incidence of 33° and working distance of about 90 mm respectively. Above the plots the polarization angles relative to the x axis with the division like in **Fehler! Verweisquelle konnte nicht gefunden werden.** are listed. Measured distributions were magnified and imaged by a 50x microscope objective onto an image sensor of 768x576 pixels with a size of 8.3 µm.

$$d_w \sim 1/tan\,\theta$$

where d_w and θ are the working distance and angle of incidence, respectively.

Fig. 2 shows that the setup covers period range of 1-5 µm, which can be calculated by equation (*3*). The period is limited by the setup for higher angles, as the beam would be cropped by the bottom of the construction. On the other hand, larger periods lead to longer working distances. Maximal goniometer configuration allows theoretically an infinite working distance. Therefore the machining area limits the variation of period. During the validation a working distance of about 750 mm was possible.

3.2. Pattern size

The size of the pattern is variable with the adjustable telescope. Fig. 2 (b) shows the possible pattern diameter versus the working distance, which is defined by the period. The blue field represents all adjustable pattern diameters. The setup is diffraction limited to smaller diameter. The large diameters are limited by the aperture of the optical elements. . This leads to maximum pattern diameters up to 5 mm for a working distance of 100 mm and 25 mm for a working distance of 750 mm.

3.3. Intensity distribution

Intensity distribution depends on the relative polarizations, which are adjustable with implemented $\lambda/2$-plates. A comparison of three simulated to measured intensity distributions are shown in Fig. 3. The calculation was made with equation (1). The scale of the simulated intensities is normed to intensities

without interference effects. Above the plots the polarization angles relative to the x axis defined in Fig. 1 are listed. The angle of incidence was 33° with a working distance of about 90 mm. The comparison shows a clear correlation between the simulation and the measurement of the intensity distributions. Over the working distance the three distributions are constant, except their period. This constancy applies not to all adjustable intensity distributions.

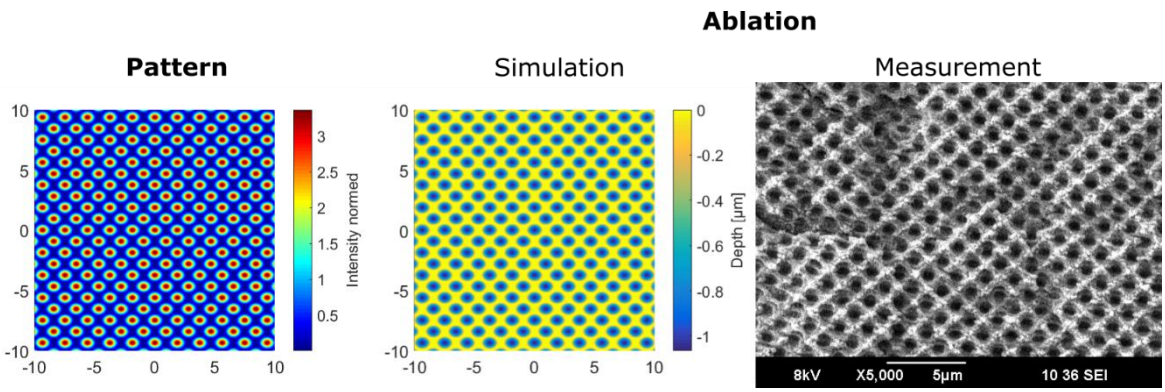

Fig, 4. Experimental verification of structuring ability. Comparison of simulated interference pattern (left) and the simulated resulting ablation by Lambert-Beer (middle) to scanning microscope (SEM) measured ablation structure after 90 pulses (right).

3.4. Experimental validation with ablation

The usability of the setup was verified with a multi – pulse ablation experiment with 90 pulses. The ablation was done with a pulse energy of 75 µJ at a repetition rate of 300 Hz to avoid heat accumulation effects. The pattern diameter was adjusted to 100 µm and the angle of incidence to 33°. The material was stainless steel with an ablation threshold of about 0.1 J/cm².

Fig, 4 shows the comparison of simulated interference pattern (left) and the simulated resulting ablation by Lambert-Beer (middle) to the SEM measured structure after processing (right). The comparison shows a clear correlation with the simulated period of 1.31 µm and measured average period of 1.32 µm of the ablated structure.

4. Conclusion

In this work a flexible and compact direct laser interference patterning (DLIP) setup based on four beam interference principle was developed and build up. The setup has a wide range of adjustment of the period, size and intensity distribution of the interference pattern. Following values were reached and verified. The period is adjustable from 1 µm up to 7 µm, limited by machining area. Pattern sizes expressed as pattern diameters of at least 70 µm and 150 µm, dependent on the period, were shown. It is possible to increase the diameter up to at most 5 mm and 25 mm, limited by the aperture. The feasibility of three different intensity distributions correlated to simulations were shown. Except the linear dependence of the pattern size to the period and a limited number of adjustable interference patterns, independent variation of these three parameters can be guaranteed.

The validation and ablation experiment was done with a picosecond laser, confirming the ability with laser pulses with less than 3 mm coherence length.

The optical setup was embedded in a compact and stable construction of 10 mm thick aluminum plates that provides a stable interference pattern during processes and standby periods, even after movement of the entire setup.

Acknowledgements

This project has received funding from the European Union's Horizon 2020 research and innovation programme under grant agreement No 687613 (www.tresclean.eu)

References

Aliekber Aktaga, Steven Michalski, Lanping Yue, Roger D. Kirby, and Sy-Hwang Liou, 2006. Formation of an anisotropy lattice in Co/Pt multilayers by direct laser interference patterning, JOURNAL OF APPLIED PHYSICS 99, 093901

Andrés LASAGNI, Dimitri BENKE, Tim KUNZE, Matthias BIEDA, Sebastian ECKHARDT, Teja ROCH, Denise LANGHEINRICH, and Jana BERGER, 2015. Bringing the Direct Laser Interference Patterning Method to Industry: a One Tool-Complete Solution for Surface Functionalization, JLMN-Journal of Laser Micro/Nanoengineering Vol. 10, No. 3

Andrés Lasagni, Teja Rochab, Matthias Biedaa, Dimitri Benkeab, Eckhard Beyerab, 2014. High speed surface functionalization using direct laser interference patterning, towards 1 m²/min fabrication speed with sub-µm resolution, Proc. of SPIE Vol. 8968, 89680A

Beat Neuenschwander, Beat Jaeggi, Marc Schmid, Vincent Rouffiange and Paul-E. Martin, 2012. Optimization of the volume ablation rate for metals at different laser pulse-durations from ps to fs, Proc. of SPIE Vol. 8243, 824307

Cheng Lu and R. H. Lipson, 2010. Interference lithography: a powerful tool for fabricating periodic structures, Laser Photonics Rev. 4, No. 4, 568–580

Jintang Huang, Stefan Beckemper, Arnold Gillner and Keyi Wang, 2010. Tunable surface texturing by polarization-controlled three-beam interference, J. Micromech. Microeng. 20

M. Campbell, D. N. Sharp, M. T. Harrison, R. G. Denning, A. J. Turberfield, 2000. Fabrication of photonic crystals for the visible spectrum by holographic lithography. NATURE, VOL 404, p. 53

Michael Steger and Arnold Gillner, 2016. Analysis and Evaluation of Boundary Conditions for Direct Surface Structuring by Multi-Beam Interference, JLMN-Journal of Laser Micro/Nanoengineering Vol. 11, No. 3